applied sciences

MDPI

Article

Gray Image Denoising Based on Array Stochastic Resonance and Improved Whale Optimization Algorithm

Weichao Huang [1,2,*], Ganggang Zhang [2], Shangbin Jiao [1] and Jing Wang [3]

[1] Shannxi Key Laboratory of Complex System Control and Intelligent Information Processing, Xi'an University of Technology, Xi'an 710048, China
[2] School of Automation and Information Engineering, Xi'an University of Technology, Xi'an 710048, China
[3] School of Printing, Packaging and Digital Media, Xi'an University of Technology, Xi'an 710048, China
* Correspondence: huangwc@xaut.edu.cn

Abstract: Aiming at the poor effect of traditional denoising algorithms on image enhancement with strong noise, an image denoising algorithm based on improved whale optimization algorithm and parameter adaptive array stochastic resonance is proposed in the paper. In this algorithm, through dimensionality reduction scanning, coding, modulation and other processing, the noise-containing gray image becomes a one-dimensional aperiodic binary pulse amplitude modulation signal suitable for a bistable stochastic resonance model. Then, the traditional whale optimization algorithm is improved in the initial solution distribution, global search ability and population diversity generalization. The improved whale optimization algorithm is applied to select the parameters of the stochastic resonance, which effectively improves the parameters self-adaptive of the array stochastic resonance model. Finally, the denoised image is obtained by demodulating, decoding and anti-scanning the stochastic resonance output. The experimental results show that compared with the array stochastic resonance method with fixed parameters and the classical image denoising method, the algorithm proposed in this paper has better performance in terms of visual effect and peak signal-to-noise ratio index, which proves the advantages and effective application of the method in image denoising.

Keywords: image denoising; improved whale optimization algorithm; array stochastic resonance; peak signal-to-noise ratio

Citation: Huang, W.; Zhang, G.; Jiao, S.; Wang, J. Gray Image Denoising Based on Array Stochastic Resonance and Improved Whale Optimization Algorithm. *Appl. Sci.* **2022**, *12*, 12084. https://doi.org/10.3390/app122312084

Academic Editor: Zhengjun Liu

Received: 28 October 2022
Accepted: 23 November 2022
Published: 25 November 2022

1. Introduction

Image is one of the important sources for people to obtain information [1]. The image data has become a vital and irreplaceable information carrier in the fields of science and technology [2], industry [3], aerospace [4], medical care [5], education [6], etc. However, in the process of generation, acquisition and transmission, the image is often disturbed by noise, which causes image quality damage, image visual effect reduction, and even seriously affects the effective transmission of information [7]. Therefore, it is of great significance for image detection and information recognition to study image denoising algorithms under strong noise [8].

At present, the classical denoising methods mainly include mean filtering, Wiener filtering, median filtering, Gaussian filtering, etc. [9]. However, In the past decade, scholars have found that the classical image denoising methods do not perform well in a strong noise environment [10]. The application of stochastic resonance (SR) theory in image processing provides another idea for image denoising [11]. SR theory can use noise energy to enhance image signal, so as to filter out noise without damaging the original image. Therefore, the image denoising method based on the SR principle has been widely studied by scholars [12].

SR was first proposed in 1981 by R. Binzi et al. in the study of glaciers in Earth's ancient meteorology [13]. With the in-depth study of stochastic resonance theory, it has been applied more and more widely, including in the field of image processing. Ye et al.

found that the combination of SR mechanism and Radon transform could extract the linear edges of objects buried in strong noise images [14]. Liu et al. applied adaptive SR to denoising binary images in strong noise, and achieved a satisfactory peak signal-to-noise ratio in the experiment [15]. Wang et al. proposed a signal processing method based on the best matching method and array SR in 2016. They improved the processing effect of array SR and analyzed the bit error rate of the system output signal [16]. With the continuous exploration and improvement of SR mechanism in weak signal detection and enhancement, it provides a steady stream of new technologies for image denoising in the field of image processing [17].

The SR mechanism makes the input signal, noise and nonlinear system achieve the best match by adjusting the structural parameters of the system. However, selection of SR structural parameters is always a difficult problem, which has a direct impact on the output of the system [18]. The adaptive SR parameters has been a research hotspot in this field [19]. At present, many researchers selecting structural parameters of SR used intelligent optimization algorithms [20], but the optimization results are prone to fall into local optimization and low computational efficiency [21]. Therefore, when optimizing the parameters of stochastic resonance, it is very important to select an appropriate intelligent optimization algorithm for image enhancement. Intelligent optimization algorithm is an intelligent technology that has emerged in recent years. It can solve complex problems in practical projects by simulating the cooperation and competition among biological groups. With the continuous development of intelligent optimization algorithms, scholars at home and abroad have proposed many new intelligent optimization algorithms. Paniri et al. proposed a multi-label feature selection method based on ant colony optimization (ACO) [22], and then proposed a novel multi-label correlation redundancy feature selection method based on ACO [23]. Liu et al. proposed a multi leader particle swarm optimization [24]. Dowlatshahi et al. proposed a grouped GSA algorithm [25]. Serkan et al. proposed an improved whale optimization algorithm based on average swarm intelligence [26]. Whale optimization algorithm (WOA) [27] is a new intelligent optimization algorithm proposed by Mirjalili et al. to simulate the hunting behavior of a humpback whale bubble net. Compared with other traditional algorithms, it has a simpler principle and a stronger optimization ability. However, the algorithm still has many shortcomings, such as the linear and random parameters set in the algorithm, which means the optimization of the algorithm is limited, and the poor diversity of the algorithm population will lead to the problem of local optimal.

In view of the above problems, the author of this paper proposed an improved whale optimization algorithm (IWOA) [28] in the previous research, and applied the algorithm to the diagnosis of bearing fault signal, which proved that the algorithm has fast convergence speed, good optimization ability and stability, and has good application in weak signal detection. Under the above research background, this paper combines intelligent optimization algorithm with array stochastic resonance for the first time, and proposes a gray image denoising method based on improved whale optimization algorithm and parameter adaptive array stochastic resonance. Firstly, the noisy gray image is converted into one-dimension aperiodic binary pulse amplitude modulation (BPAM) signal by scanning, coding and modulating. Then, the traditional whale optimization algorithm is improved in the initial solution distribution, global search ability and population diversity generalization. The IWOA algorithm is applied to select the structural parameters of the SR. Finally, the denoised one-dimensional aperiodic signal is demodulated, decoded and reverse scanned to obtain the denoised image. Experimental results show that the proposed algorithm has an obvious effect on removing strong noise interference in image information. Comparing with the classical image denoising algorithm and the array SR algorithm with fixed parameters, the proposed algorithm has higher image quality, better visual effects and a higher peak signal-to-noise ratio.

The remaining chapters of this paper are arranged as follows: in this study, the theoretical analysis of array stochastic resonance is introduced in Section 2, and the theoretical analysis of improved whale optimization algorithm is introduced in Section 3. In Section 4,

the above two theories are combined to propose the algorithm proposed in this study. Then, in Section 5 of the article, an experimental demonstration is conducted and the experimental results are explained. Finally, in the sixth section, a summary of the full text is made.

2. Array Stochastic Resonance Principle

2.1. Bistable Stochastic Resonance

In the study of stochastic resonance theory, bistable system is one of the most commonly used models [29], which can be described by Langevin equation, namely

$$\frac{dx}{dt} = ax - bx^3 + s(t) + \xi(t) \tag{1}$$

where, a and b are the structural parameters of the bistable system, and $a > 0$, $b > 0$. $s(t)$ is the external input signal, $\xi(t)$ is the noise signal with mean value of 0 and intensity of D. When there is no input signal and noise in the system, namely $s(t) = 0$, $\xi(t) = 0$, the theoretical model expression is as follows.

$$U(x) = -\frac{a}{2}x^2 + \frac{b}{4}x^4 \tag{2}$$

where, when $x = \pm\sqrt{a/b}$, the bistable potential function is in a stable state. When $x = 0$, it is unstable, and its barrier height is $\Delta U = a^2/4b$. The potential function curve of bistable state is shown in Figure 1.

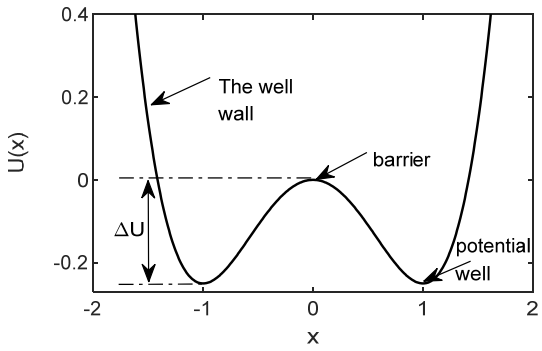

Figure 1. Potential function diagram of classical bistable model.

When the external periodic signal excitation exists and the noise intensity is zero, the relative barrier of the bistable potential well will rise and fall periodically under the periodic excitation. But at this time, the energy obtained by the particle is not enough to realize the reciprocating transition between the two potential wells. When noise intensity is not zero and external periodic excitation is zero, the particle transitions between two potential wells according to Kramers transition rate [30], and the expression of transition rate γ_k is as follows:

$$\gamma_k = \frac{a}{\sqrt{2\pi}} \exp(-\frac{\Delta U}{D}) \tag{3}$$

When a certain intensity of noise is added to the bistable system, the particle can obtain enough energy to complete the transition between the double potential wells of the system under the combined action of periodic excitation and noise. At this time, the output of the system is enhanced by transferring the energy of the noise to the weak input signal.

2.2. Array Stochastic Resonance Theory

In 2006, Duan et al. proposed the array SR theory [31] and proved that with the increase of the number of arrays, the output peak signal to noise ratio of the system will gradually increase, surpassing the input peak signal-to-noise ratio. According to the performance of the array stochastic resonance system, the application of stochastic resonance theory

in weak signal detection and extraction can be further improved. The structure of array bistable SR is shown in Figure 2.

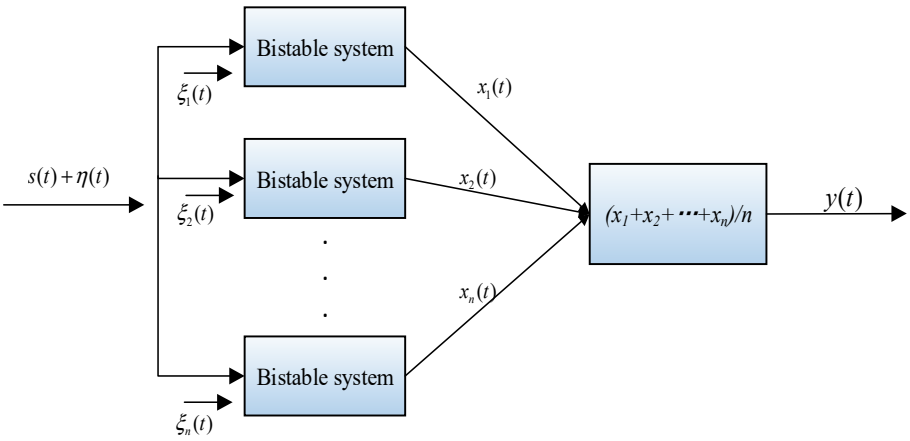

Figure 2. The structure of array bistable stochastic resonance system.

It can be seen from Figure 2 that the input of each bistable array unit is a mixed signal of the same original input $s(t)$ and noise $\eta(t)$. $\eta(t)$ refers to white Gaussian noise with mean value of 0 and noise intensity of D. $\xi_i(t)$ refers to the internal noise of each bistable array subsystem. Each subsystem in the array can be represented by Langevin equation, that is

$$\frac{dx_i}{dt} = ax_i - bx_i^3 + s(t) + \eta(t) + \xi_i(t) \tag{4}$$

where, $x_i(t)$ is the output of each array stochastic resonance subsystem, and $y(t)$ is the output of SR systems, that is

$$y(t) = \frac{1}{N}\sum_{i=1}^{N} x_i(t) \tag{5}$$

3. Improved Whale Optimization Algorithm

3.1. Whale Optimization Algorithm

A new heuristic search algorithm—Whale optimization algorithm (WOA) was proposed by Australian scholar Mirjalili in 2016. The main idea of the algorithm is to solve the target problem by imitating the predatory behavior of whales. It mainly includes three stages: surround prey, bubble net [32] and search prey. As a new swarm intelligent optimization algorithm inspired by whale predation, the whale optimization algorithm has a simple structure and requires less parameters to be adjusted. The position of each whale represents one of the feasible solutions of the WOA. The optimization problem is constantly optimized by simulating whale predation behavior. Then, the optimal individual is obtained at last and can be used as the optimal solution of the optimization problem. Whale optimization algorithm has been successfully applied to solving many parameters' optimization problems due to its simple structure and fewer parameters to be adjusted [33]. However, as a new member of the group optimization algorithm, the traditional WOA also has some common problems of the group optimization algorithm, that is, it is easy to fall into the local optimal solution, the convergence speed is slow, the convergence accuracy is low, and there are still some limitations in solving some practical problems.

3.2. Improve Whale Optimization Algorithm

As the traditional whale optimization algorithm has the problem of slow convergence and easy to fall into local optimization, this paper makes the following improvements to the whale optimization algorithm and proposes an improved whale optimization algorithm.

3.2.1. Iterative Map Initialization

The traditional WOA initializes the population in a random manner, resulting in a relatively uneven distribution of the initial population. The research shows that the chaotic sequence has good randomness and ergodicity, so this paper adopts the method of iterative mapping to initialize the population, and its equation is as follows

$$x_{k+1} = \sin(d\pi/x_k) \tag{6}$$

where, d is the control parameter, $d \in (0,1)$, and $d = 0.5$ is taken in the paper, x_k is the current whale position, k is the current number of iterations.

3.2.2. Nonlinear Convergence Factor and Variable Weight

In the traditional whale optimization algorithm, the convergence factor decreases linearly from 2 to 0 as the number of evolutionary iterations increases, but WOA algorithm changes nonlinearly in the evolutionary search process. The linear decrease strategy of the convergence factor cannot fully reflect the actual optimization search process of the algorithm. To solve this problem, this paper proposes a nonlinear change strategy of convergence factor v' with the number of evolution iterations, namely

$$\begin{cases} v' = 1 + \cos(\pi \times \frac{t}{T}), & t \le 0.5T \\ v' = \cos(\pi \times \frac{t-0.5T}{T}), & t > 0.5T \end{cases} \tag{7}$$

The value of nonlinear time-varying factor v' changes dynamically with the number of iterations. The initial v' value of the algorithm is large, which increases the step size of the global optimization stage of the algorithm, effectively expands the scope of the algorithm for global search, and enhances the global performance of the algorithm. In the middle of the algorithm, local development is carried out after the suspected target is determined. At this time, the larger v' value enables the algorithm to have a larger step size, effectively enhancing the ability of the algorithm to jump out of the local extreme value, and avoiding the algorithm from falling into local optimization. In the later stage of the algorithm, when approaching the optimal solution, the convergence speed of the v' value becomes slower, making the algorithm have a smaller step size, which is conducive to a local fine search and stable optimization, effectively improving the convergence speed of the algorithm. Therefore, the nonlinear time-varying factor v' can more reasonably balance the global exploration in the early stage and the local exploitation in the middle and late stage of the algorithm without changing the segmentation point of the global exploration and local exploitation.

Because in the traditional whale optimization algorithm, the position of new individuals generated in each iteration only depends on the current target individual position and the global optimal individual position. Therefore, it is easy to cause the algorithm to fall into local optimum. This paper designs a variable weight strategy for this purpose, namely

$$w(t) = \frac{2}{\pi} \times \tan(\frac{t}{T}) \tag{8}$$

The improved location update formula is as follows

$$\vec{X}(t+1) = \vec{X_{rand}} \times w - \vec{A} \cdot \vec{E}_{rand}, p < 0.5, |A| > 1 \tag{9}$$

$$\vec{X}(t+1) = \vec{X}^*(t) \times w - \vec{A} \cdot \vec{E}, p < 0.5, |A| \le 1 \tag{10}$$

$$\vec{X}(t+1) = \vec{E'}(t) e^{ml} \cos(2\pi l) + \vec{X}^*(t) \times (1-w), p \ge 0.5 \tag{11}$$

With the increase of the number of iterations, the weights in the variable weight strategy increase nonlinearly. Since the target of individual whale is fuzzy at the initial stage of search, a smaller weight is used to perturb the current optimal solution position.

In the middle and late stages of the iteration, the target of the whale is gradually clear. At this time, the current optimal position is disturbed with a large weight to achieve the goal of fine search and rapid convergence in the optimal solution field.

3.2.3. Random Learning Strategy

The quality of whale population has a great impact on the performance of the traditional whale optimization algorithm. High quality whale population can improve the algorithm's optimization performance and speed up the algorithm's convergence while improving the algorithm's accuracy. Because the traditional whale optimization algorithm only relies on the guidance of random individuals in the population to update the individual position during global search, the learning phase of the teaching and learning optimization algorithm is introduced, and a random learning strategy [34] is proposed to simulate the learning mode of discussion and communication between whales. By learning from excellent individuals, the self-position is optimized, and the social learning ability of the whale population is increased, thus increasing the diversity of the whale population, and improving the whale population quality to improve the global search performance of the algorithm. As shown in Formula (12), for whale individual x, different individuals x_p are randomly selected from the whale population and learned from them to adjust their positions.

$$x_{new} = \begin{cases} x + rand(0,1) \times (x - x_p), f(x_p) < f(x) \\ x + rand(0,1) \times (x_p - x), f(x_p) > f(x) \end{cases} \tag{12}$$

where the learning factor $rand(0,1)$ is a random number between (0,1), which reflects the difference in learning ability of whale individuals. After learning, a better individual was selected by comparing fitness values. If $f(x_{new}) < f(x)$, the population will accept the new individual x_{new} and replace individual x, otherwise the population will reject the inferior individual x_{new}. The randomness learning of individuals enhances the information sharing ability of the whale population, thus increasing the diversity of the population and improving the performance of the algorithm for global optimization.

3.2.4. Cauchy Mutation Strategy

For the problem that the traditional whale optimization algorithm is easy to fall into local extremum, the Cauchy mutation strategy is introduced in combination with Cauchy distribution to give the current optimal individual Cauchy perturbation. In the later stage of the algorithm, Cauchy operator can generate a larger step size to help the algorithm jump out of the local optimum, and can also generate a smaller step size to speed up the search for the optimal solution. Therefore, the following Cauchy variation formula is adopted to update the position of the current optimal individual, namely

$$x^*_{new}(t) = x^*(t) \times (1 + cauchy(0,1)) \tag{13}$$

where, $x^*_{new}(t)$ is the new value obtained from the current optimal value after Cauchy perturbation, $cauchy(0,1)$ is the Cauchy operator, and the standard Cauchy distribution function formula [35] is

$$f(x) = \frac{1}{\pi \times (x^2 + 1)}, x \in (-\infty, +\infty) \tag{14}$$

Because Cauchy probability density function has a wide distribution range and can generate random numbers far from the origin, it can impose strong disturbances on whale individuals, so that the disturbed whales can quickly avoid local optima. At the same time, due to the low peak value of Cauchy distribution, the individual search time is greatly shortened, so that the algorithm can converge faster.

4. Array Stochastic Resonance Strategy Based on Improved Whale Optimization Algorithm

4.1. Image Denoising Method by Array Stochastic Resonance

4.1.1. Image Dimension Reduction Coding

The original gray image $T_{m\times n}$ is dimensionality reduction scanning by the Hilbert scanning mode [36] in the paper. The original two-dimensional image matrix $T_{m\times n}$ is scanning into a one-dimensional image sequence $J_{1\times mn}$. Because the encoding and decoding operations of the binary encoding method are simple and easy, and conform to the minimum character set encoding principle, we encode the one-dimensional image sequence $J_{1\times mn}$ to obtain an 8-bit binary symbol sequence $H_{1\times 8mn}$ composed of 0 and 1.

4.1.2. Modulation

The binary pulse amplitude modulation (BPAM) is applied to binary symbol sequence $H_{1\times 8mn}$ to obtain a one-dimensional bipolar aperiodic BPAM signal $r(t)$. The formula is as follows

$$r(t) = A\sum_{i=1}^{8mn} S_i G(t - iT) \tag{15}$$

where A is the amplitude of signal $r(t)$, m and n are the rows and columns of the original grayscale image. $G(t)$ is a rectangular pulse with a period of T, when $t \in (0, T)$, $G(t)$ is 1, and when $t \notin (0, T)$, $G(t)$ is 0. $S_i(i = 1, 2, \cdots, 8mn)$ is a one-dimensional sequence consisting of -1 and 1 obtained by the polarity conversion of binary sequence $H_{1\times 8mn}(0 \to -1, 1 \to 1)$. Through image dimension reduction scanning, binary symbol coding and image symbol polarity conversion, a one-dimensional sequence S_i is obtained, that is, all information on S_i is independent random variables.

4.1.3. Array Saturation Stochastic Resonance Process

The core of image processing is the array stochastic resonance structure, and each independent sub array can be regarded as an image channel. Its input is the noisy signal $r(t) = s(t) + \eta(t)$ obtained from the original gray image through a series of changes such as dimension reduction, coding and modulation. The output of each bistable array subsystem is $x_n(t), n = 1, 2, \cdots, L$, where n is the number of array elements. The overall output response of an array stochastic resonance system can be regarded as the arithmetic mean sum of each subarray, namely

$$x(t) = \sum_{n=1}^{L} x_n(t)/L \tag{16}$$

4.1.4. Demodulation

Set the start time of each symbol S_i to $t_i = iT$ and the duration to T. The demodulation method for the output response $x(t)$ of the array saturated stochastic resonance system is

$$P(t) = sign(x(t_i + T)) = \begin{cases} 1 \; x(t_i + T) \geq 0 \\ 0 \; x(t_i + T) < 0 \end{cases} \tag{17}$$

The demodulated one-dimensional binary signal $P_{1\times 8mn}$ is decoded into decimal symbols to obtain one-dimensional sequence $V_{1\times mn}$.

Then, the one-dimensional sequence $V_{1\times mn}$ is inverse scanned to the restored gray image Q_{mn}.

4.2. Array Stochastic Resonance Strategy Based on Improved Whale Optimization Algorithm

The peak signal-to-noise ratio (PSNR) is an important means to evaluate images in common use, and is an important evaluation index of image processing performance in most image processing. The value of PSNR is proportional to the image quality. The PSNR

is used to evaluate the image denoising effect of the proposed algorithm. The PSNR can be expressed as

$$\mathrm{MSE} = \frac{1}{mn}\sum_{i=0}^{m-1}\sum_{j=0}^{n-1}\|X(i,j) - Y(i,j)\|^2 \tag{18}$$

$$\mathrm{PSNR} = 10 * \log_{10}(\frac{(2^n-1)^2}{\mathrm{MSE}}) \tag{19}$$

where MSE represents the Mean Square Error [37] of the denoised image X and the original input image Y, and n is the number of bits per pixel. The larger the PSNR, the smaller the gap with the original input image, and the higher the image quality.

For WOA whose population size is N, the problem dimension is dim, and the maximum number of iterations is Max_iter; the complexity calculation method is

$$\mathrm{O(WOA)} = \mathrm{O(N \cdot dim \cdot Max\_iter)} \tag{20}$$

For array stochastic resonance with gray image pixel size $m \cdot n$ and array element number L, the complexity calculation method is

$$\mathrm{O(Array\ SR)} = \mathrm{O(m \cdot n \cdot 8 \cdot 102 + L)} \tag{21}$$

The computational complexity of parameter adaptive array model method based on WOA is as follows

$$\mathrm{O(N \cdot dim \cdot Max\_iter \cdot (m \cdot n \cdot 8 \cdot 102 + L))} \tag{22}$$

IWOA algorithm adopts the iterative mapping method to initiate the iterative population. In array stochastic resonance, the pixel size of gray image is $m \cdot n$ and the number of array units is L. Therefore, the complexity calculation method of the proposed algorithm is

$$\mathrm{O(this\ paper)} = \mathrm{O(N^2 \cdot dim \cdot Max\_iter \cdot (m \cdot n \cdot 8 \cdot 102 + L))} \tag{23}$$

It can be seen from the above analysis that the computational complexity of the algorithm proposed in this paper is greater than that of array stochastic resonance and WOA based parametric adaptive array model methods.

The process of the algorithm proposed in this paper is shown in Figure 3. Firstly, the image with noise is processed by gray scale mapping and dimensionality reduction scanning to meet the requirements of the stochastic resonance input signal. The processed image signal is used as the input signal of the bistable stochastic resonance model, and the fourth order Runge-Kutta method is used to solve the problem numerically. Then, the negative number of PSNR is taken as the fitness function of IWOA, and the optimal position is updated according to the principle that the minimum value of the fitness function corresponds to the optimal position. The operation is repeated until the maximum number of iterations, and the minimum fitness function value is selected. At this time, the parameter combinations a, b and h are taken as the optimal parameter combination of the system. Finally, the optimal parameter combination is brought into the system for solving, and the final image of array random resonance processing is obtained.

4.3. Parameter Analysis of Improved Whale Optimization Algorithm

The global search ability and local search ability of whale optimization algorithm largely depends on the value of parameter A, which changes with the convergence factor v'. At the initial stage of the search, the target of whale individuals is fuzzy. At this time, a large v' value is used to increase the probability that $|A|$ value is greater than 1, thus increasing the step size of the algorithm in the global optimization stage. Learning factors are introduced to increase the diversity of whale populations, effectively expanding the scope of the algorithm for global search. In the middle of the algorithm, local development is carried out after the suspected target is determined. At this time, the larger v' value

makes the algorithm have a larger step size, and perturbs the current optimal position with a larger weight, effectively enhancing the ability of the algorithm to jump out of the local extreme value, and avoiding the algorithm from falling into local optimization. In the later stage of the algorithm, when approaching the optimal solution, the convergence speed of the v' value becomes slower. At this time, the fluctuation amplitude of the $|A|$ value is significantly weakened, so that the algorithm has a smaller step size, and perturbs the current optimal position with a large weight. At the same time, Cauchy operator is introduced to help the algorithm jump out of the local optimization and speed up the search for the optimal solution. The setting of these parameters is conducive to local fine search and stable optimization, and effectively improves the convergence speed of the algorithm.

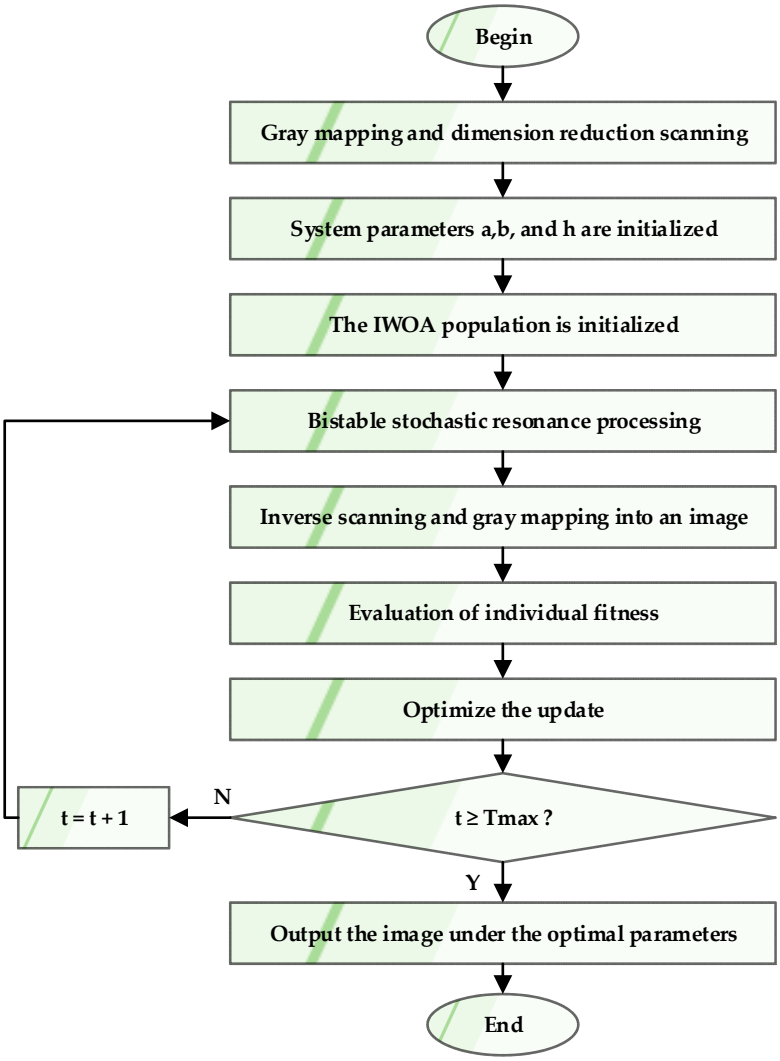

Figure 3. Flow chart of array SR based on IWOA.

5. Image Denoising Based on Array Stochastic Resonance and Improved Whale Optimization Algorithm

Based on Intel (R) Core (TM) i5-7200U CPU, 2.5 GHz main frequency, 16 GB memory and Windows 10 (64 bit) operating system, this paper conducts simulation experiments on the proposed algorithm. The programming software is MATLAB R2021b. In order to verify the correctness of the method presented in this paper, Lena image, Baboon image and Magnetic resonance imaging (MRI) image with white Gaussian noise were respectively subjected to group denoising experiments. In the experiment, the image restoration performance of the array model method [38] with fixed parameters (FP), the

parameter adaptive array model method based on WOA and the parameter adaptive array model method based on IWOA proposed in this paper are compared.

5.1. Lena Image

A Lena grayscale image with pixel size of 256 × 256 was used for testing. The noise is Gaussian white noise with a mean value of 0 and an intensity of 0.3. Figure 4 shows the Lena gray image, the Lena noise image, and the denoising Lena image by mean method, median method, Wiener method and Gaussian method. It can be seen from the Figure 4 that in the strong noise environment, the restored image processed by the mean method, median method, Wiener method and Gaussian method has been seriously distorted, resulting in the blurring of the basic content of the image.

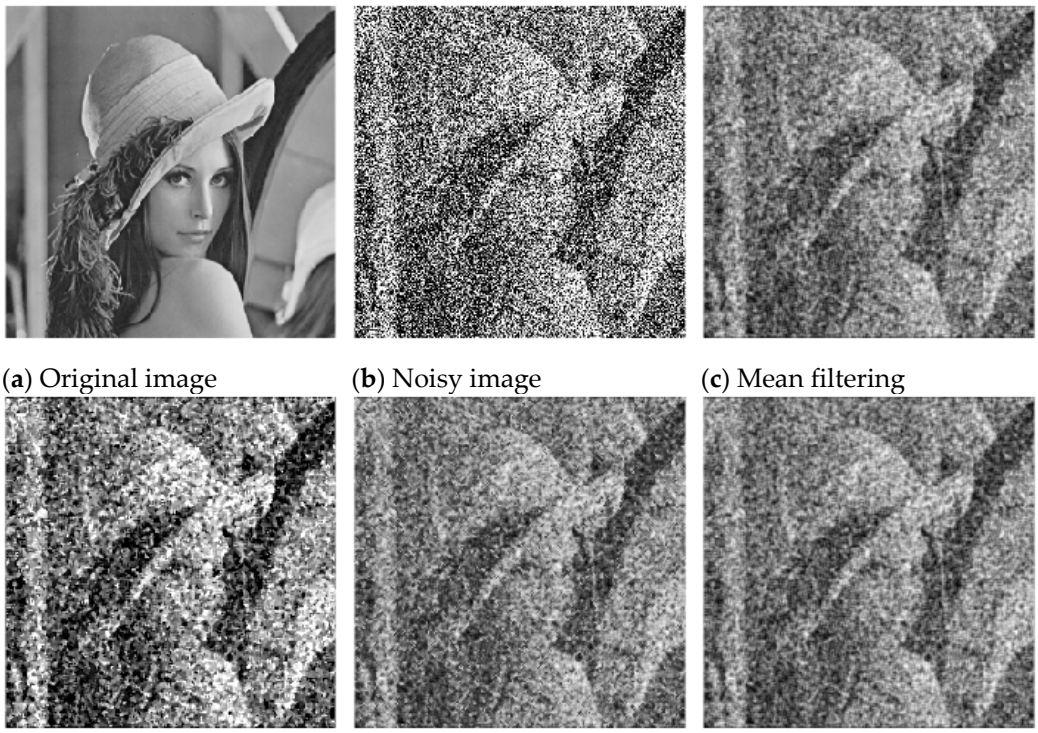

(**a**) Original image (**b**) Noisy image (**c**) Mean filtering

(**d**) Median filtering (**e**) Wiener filtering (**f**) Gaussian filtering

Figure 4. Lena image enhancement for four classical filtering methods.

The comparison of PSNR performance of mean filtering, median filtering, Wiener filtering and Gaussian filtering methods is shown in Table 1. Compared with the PSNR of noise Lena image, the PSNR of the four classical filtering methods is slightly increased, but as the increase is not more than two times, the enhancement effect is not obvious, and the image will become blurred after restoration. This means that the four classical filtering methods do not perform well in image restoration and cannot restore the image well.

Table 1. Lena image under four classical filtering algorithms for PSNR (dB).

Image Name	Size	Noisy Image	Mean	Median	Wiener	Gaussian
Lena	256 × 256	8.7167	16.6138	13.3217	15.9101	16.6173

The denoising results of the array SR with fixed parameters, the parameter adaptive array SR based on WOA and our method on Lena image at the array number are N = 1, 2, 4, 8, as shown in Figure 5. It can be seen from Figure 5 that when the array unit is small, there are many noise points on the restored image, resulting in the poor visual effect of the image. With the increase of array units, the image restoration effect is enhanced, and the image is

clearer. Furthermore, among the restored Lena images processed by three model methods, the restored image processed by the IWOA-based parameter adaptive array model method proposed in this paper is the closest to the original image, which can better show the gray level and image content of the original image. Through comparing the denoising results of the above three methods, it can be clearly seen that our method proposed in this paper has the best denoising effect, which can better show the gray level and image content of the original image.

(**a**) Array N = 1 (FP) (**b**) Array N = 1 (WOA) (**c**) Array N = 1 (IWOA)

(**d**) Array N = 2 (FP) (**e**) Array N = 2 (WOA) (**f**) Array N = 2 (IWOA)

(**g**) Array N = 4 (FP) (**h**) Array N = 4 (WOA) (**i**) Array N = 4 (IWOA)

(**j**) Array N = 8 (FP) (**k**) Array N = 8 (WOA) (**l**) Array N = 8 (IWOA)

Figure 5. Comparison of denoising effect of Lena image.

The comparison results of PSNR of the above three methods are shown in Table 2. The empirical parameters a, b and h are selected for the array SR with fixed parameters, and the obtained PSNR is slightly larger than that of the traditional denoising method. The PSNR of the denoising result is greatly improved by whale optimization of the adaptive parameter SR. The proposed IWOA parametric adaptive array SR has the largest PSNR under different array numbers, and the enhancement of PSNR value is the largest when the array number is 8, increasing by 32.4266 dB. It can be seen that the parameter adaptive array model method proposed in this paper based on IWOA has better denoising ability.

Table 2. Lena image PSNR under different array saturation model methods (dB).

	Array Unit N = 1	**Array Unit N = 2**	**Array Unit N = 4**	**Array Unit N = 8**
Fixed parameters	PSNR = 12.0409 a = 0.5; b = 1.5; h = 0.12	PSNR = 13.7994 a = 0.5; b = 1.5; h = 0.12	PSNR = 17.0191 a = 0.5; b = 1.5; h = 0.12	PSNR = 22.9659 a = 0.5; b = 1.5; h = 0.12
WOA optimization	PSNR = 15.5079 a = 0.53; b = 0.64; h = 0.06	PSNR = 19.607 a = 0.5; b = 3.14; h = 0.03	PSNR = 26.7732 a = 0.5; b = 0.86; h = 0.06	PSNR = 40.5919 a = 0.5; b = 1.05; h = 0.06
IWOA optimization	PSNR = 15.5679 a = 0.5; b = 1.21; h = 0.05	PSNR = 26.4684 a = 0.57; b = 0.48; h = 0.08	PSNR = 26.9934 a = 0.52; b = 1.17; h = 0.05	PSNR = 41.1433 a = 0.5; b = 0.67; h = 0.07

5.2. Baboon Image

A Baboon grayscale image with pixel size of 256 × 256 was used for testing. The noise is Gaussian white noise with a mean value of 0 and an intensity of 0.3. Figure 6 shows the Baboon grayscale image, the Baboon noise image, and the denoising Baboon image by mean method, median method, Wiener method and Gaussian method. As can be seen from the Figure 6, the traditional filtering algorithms make it difficult to remove the strong noise in the image. The PSNR performance after noisy Baboon image enhancement is shown in Table 3. As can be seen from Table 3, the PSNR of the restored image obtained by the four classical filtering methods is all small, the increase is not more than two times, the enhancement effect is not obvious, and the restored image will become fuzzy.

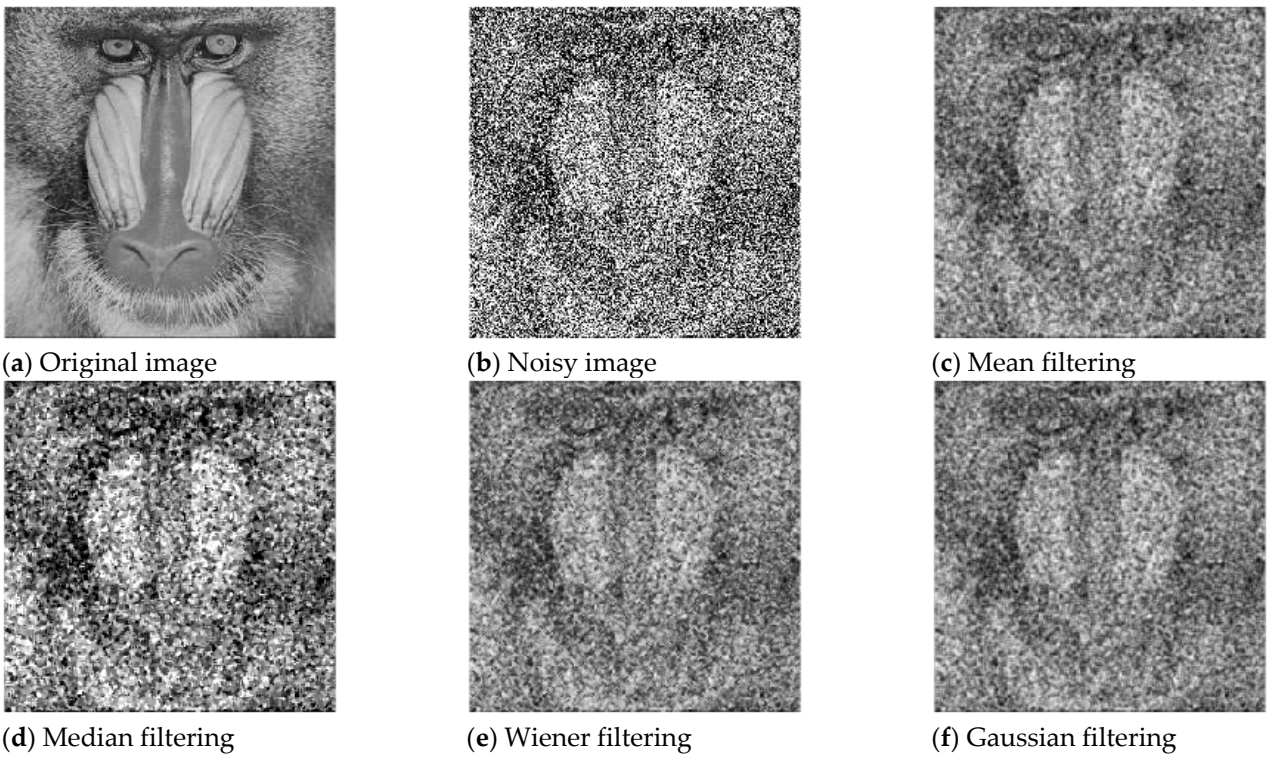

(**a**) Original image (**b**) Noisy image (**c**) Mean filtering

(**d**) Median filtering (**e**) Wiener filtering (**f**) Gaussian filtering

Figure 6. Baboon image enhancement for four classical filtering methods.

Table 3. Baboon image under four classical filtering algorithms for PSNR (dB).

Image Name	Size	Noisy Image	Mean	Median	Wiener	Gaussian
Baboon	256×256	8.6783	16.5892	12.9568	15.9909	16.6008

Under different array element sizes, the restored images obtained by the array model method with fixed parameters (FP), the parameter adaptive array model method based on WOA and the parameter adaptive array model method based on IWOA proposed in this paper are shown in Figure 7. It can be seen from Figure 7 that with the increase of array unit size, the noise spots on the denoising image are reduced obviously by the three methods. Among them, under different array unit sizes, the denoising images obtained by our method are the clearest. When the array unit size is 8, the denoising image by our method is very similar to the original image, with only a few noise points.

The comparison results of PSNR of the above three methods are shown in Table 4. In Table 4, when the number of arrays is 1, the PSNR of restored images obtained by the array model method with fixed parameters, the parameter adaptive array model method based on WOA and the parameter adaptive array model method based on IWOA proposed in this paper all increase, but the increase is small, and the image enhancement effect is still unclear. With the increase of the number of array elements, the PSNR of the restored image also increases, which makes the image restoration effect clearer. Moreover, in each array element, the PSNR of the restored image obtained by the IWOA-based parameter adaptive array model method is the maximum, which indicates that the method proposed in this paper has significant advantages in the process of gray image restoration.

Table 4. Baboon image PSNR under different array saturation model methods (dB).

	Array Unit N = 1	Array Unit N = 2	Array Unit N = 4	Array Unit N = 8
Fixed parameters	PSNR = 12.2744 a = 0.5; b = 1.5; h = 0.12	PSNR = 13.9195 a = 0.5; b = 1.5; h = 0.12	PSNR = 16.9321 a = 0.5; b = 1.5; h = 0.12	PSNR = 22.9212 a = 0.5; b = 1.5; h = 0.12
WOA optimization	PSNR = 15.3704 a = 0.5; b = 0.12; h = 0.12	PSNR = 19.3184 a = 0.58; b = 0.80; h = 0.06	PSNR = 25.926 a = 0.51; b = 0.19; h = 0.11	PSNR = 41.6294 a = 0.5; b = 5.00; h = 0.03
IWOA optimization	PSNR = 15.5307 a = 0.5; b = 1.37; h = 0.04	PSNR = 19.4159 a = 0.61; b = 3.23; h = 0.03	PSNR = 26.9586 a = 0.5; b = 4.88; h = 0.03	PSNR = 41.6387 a = 0.51; b = 1.25; h = 0.05

5.3. Magnetic Resonance Imaging Image

An MRI grayscale image with pixel size of 256 × 256 was used for testing. The noise is Gaussian white noise with a mean value of 0 and an intensity of 0.3. Figure 8 shows the MRI grayscale image, the MRI noise image, the denoising MRI image by mean method, median method, Wiener method and Gaussian method. The PSNR performance comparison results of the processed MRI images are shown in Table 5. As can be seen from Table 5, compared with the PSNR of noisy MRI images, the PSNR value of MRI images after mean filtering, median filtering, Wiener filtering and Gaussian filtering is small, the PSNR value improvement effect is not obvious, and the image enhancement effect is not good.

Table 5. MRI image under four classical filtering algorithms for PSNR (dB).

Image Name	Size	Noisy Image	Mean	Median	Wiener	Gaussian
Brain	256 × 256	8.6885	15.6739	14.1595	14.9413	15.6747

The image enhancement effect based on the array model method is shown in Figure 9. It can be seen from Figure 9 that with the increase of array unit size, the noise black and white spots on the restored image of the fixed parameter array model method, the parameter adaptive array model method based on WOA and the parameter adaptive array

model method based on IWOA proposed in this paper become less and less, and the restored image gradually becomes clearer. Among them, under different array unit sizes, the restored images obtained by the parameter adaptive array model method based on IWOA proposed in this paper are the clearest. When the array unit size is 8, the restored image obtained by the IWOA-based parameter adaptive array model method proposed in this paper is very similar to the original image, with only a few noise points.

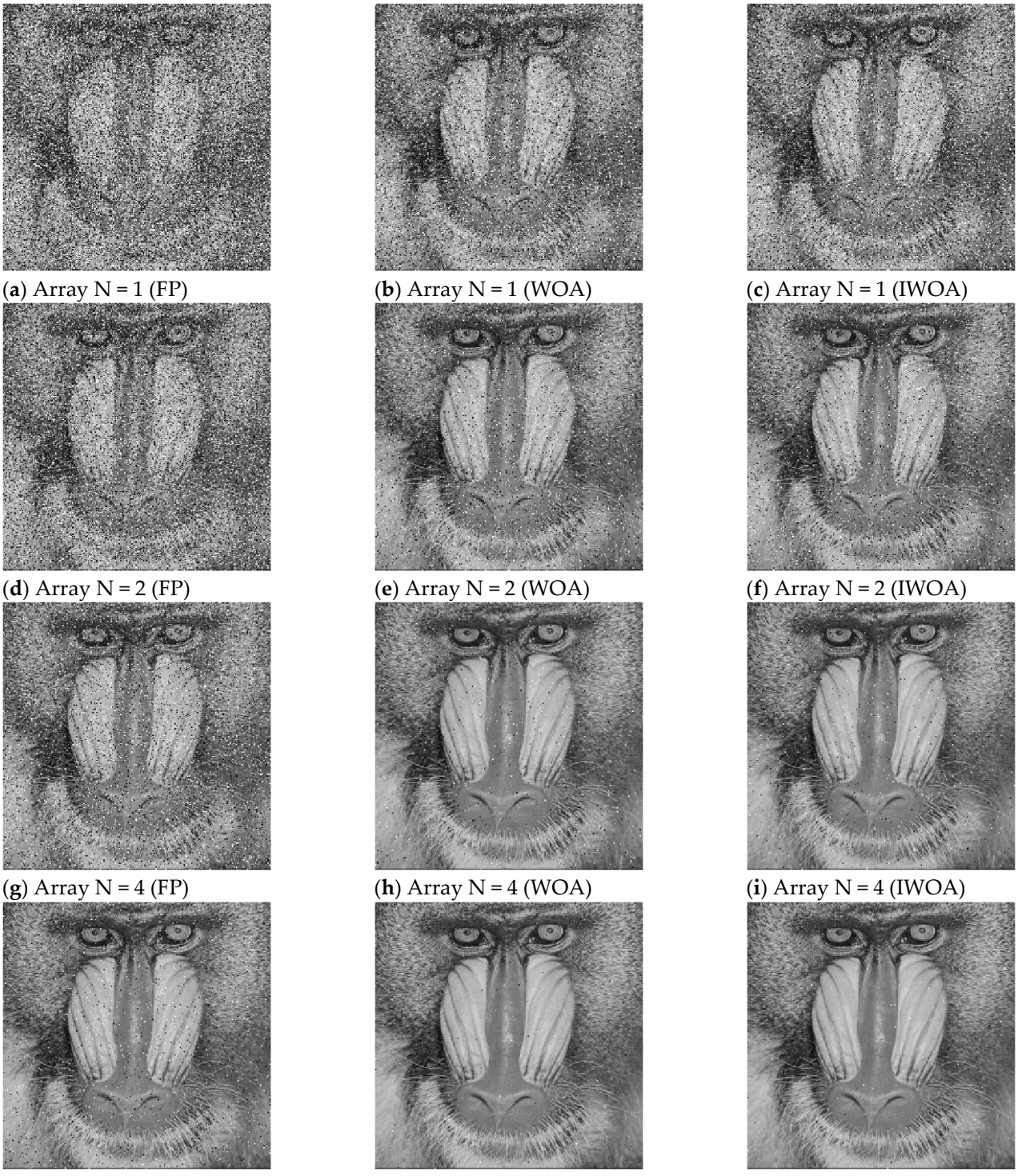

(**a**) Array N = 1 (FP) (**b**) Array N = 1 (WOA) (**c**) Array N = 1 (IWOA)

(**d**) Array N = 2 (FP) (**e**) Array N = 2 (WOA) (**f**) Array N = 2 (IWOA)

(**g**) Array N = 4 (FP) (**h**) Array N = 4 (WOA) (**i**) Array N = 4 (IWOA)

(**j**) Array N = 8 (FP) (**k**) Array N = 8 (WOA) (**l**) Array N = 8 (IWOA)

Figure 7. Comparison of denoising effect of Baboon image.

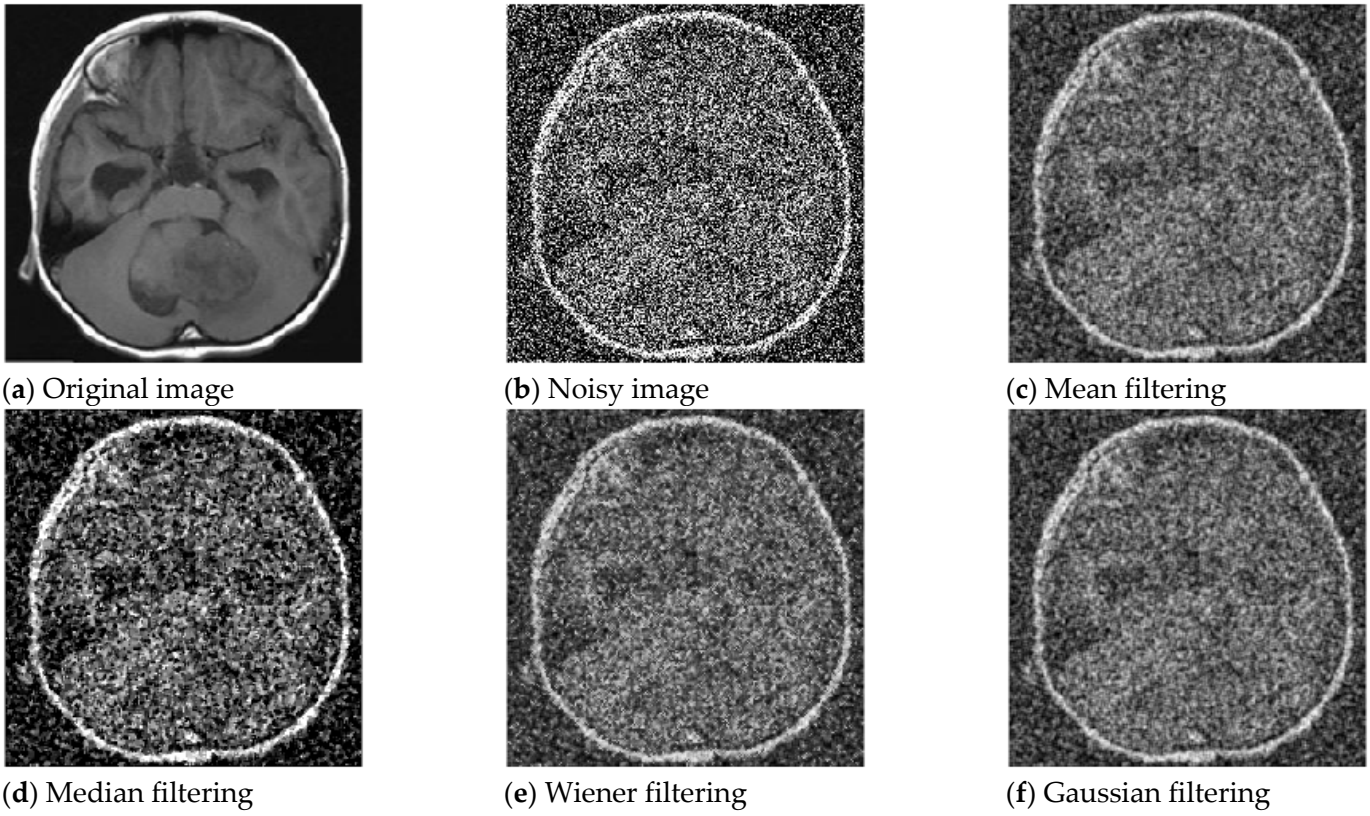

(**a**) Original image (**b**) Noisy image (**c**) Mean filtering

(**d**) Median filtering (**e**) Wiener filtering (**f**) Gaussian filtering

Figure 8. MRI image enhancement for four classical filtering methods.

The comparison results of PSNR of the above three methods are shown in Table 6. As can be seen from Table 6, when the number of arrays is 1, the PSNR value obtained by the three model methods for image restoration is relatively small, and the processing effect is not good. With the increase of the size of the array element, the PSNR of the restored image of the three model methods also increases, so that the image restoration effect is better. Moreover, the PSNR value of the restored image of the IWOA-based parameter adaptive array model method proposed in this paper is the largest, and the image enhancement effect is the best. Experimental results show that the proposed IWOA-based parametric adaptive array model method has significant advantages in image enhancement.

Table 6. MRI image PSNR under different array saturation model methods (dB).

	Array Unit N = 1	**Array Unit N = 2**	**Array Unit N = 4**	**Array Unit N = 8**
Fixed parameters	PSNR = 11.5700 a = 0.5; b = 1.5; h = 0.12	PSNR = 13.4826 a = 0.5; b = 1.5; h = 0.12	PSNR = 16.7897 a = 0.5; b = 1.5; h = 0.12	PSNR = 22.9187 a = 0.5; b = 1.5; h = 0.12
WOA optimization	PSNR = 15.4988 a = 0.5; b = 0.99; h = 0.05	PSNR = 19.6323 a = 0.5; b = 2.47; h = 0.03	PSNR = 26.6149 a = 0.5; b = 0.31; h = 0.09	PSNR = 41.1891 a = 0.5; b = 0.69; h = 0.07
IWOA optimization	PSNR = 15.5083 a = 0.51; b = 0.60; h = 0.06	PSNR = 19.6695 a = 0.5; b = 1.59; h = 0.04	PSNR = 26.6260 a = 0.57; b = 0.49; h = 0.08	PSNR = 42.3748 a = 0.64; b = 3.32;h = 0.04

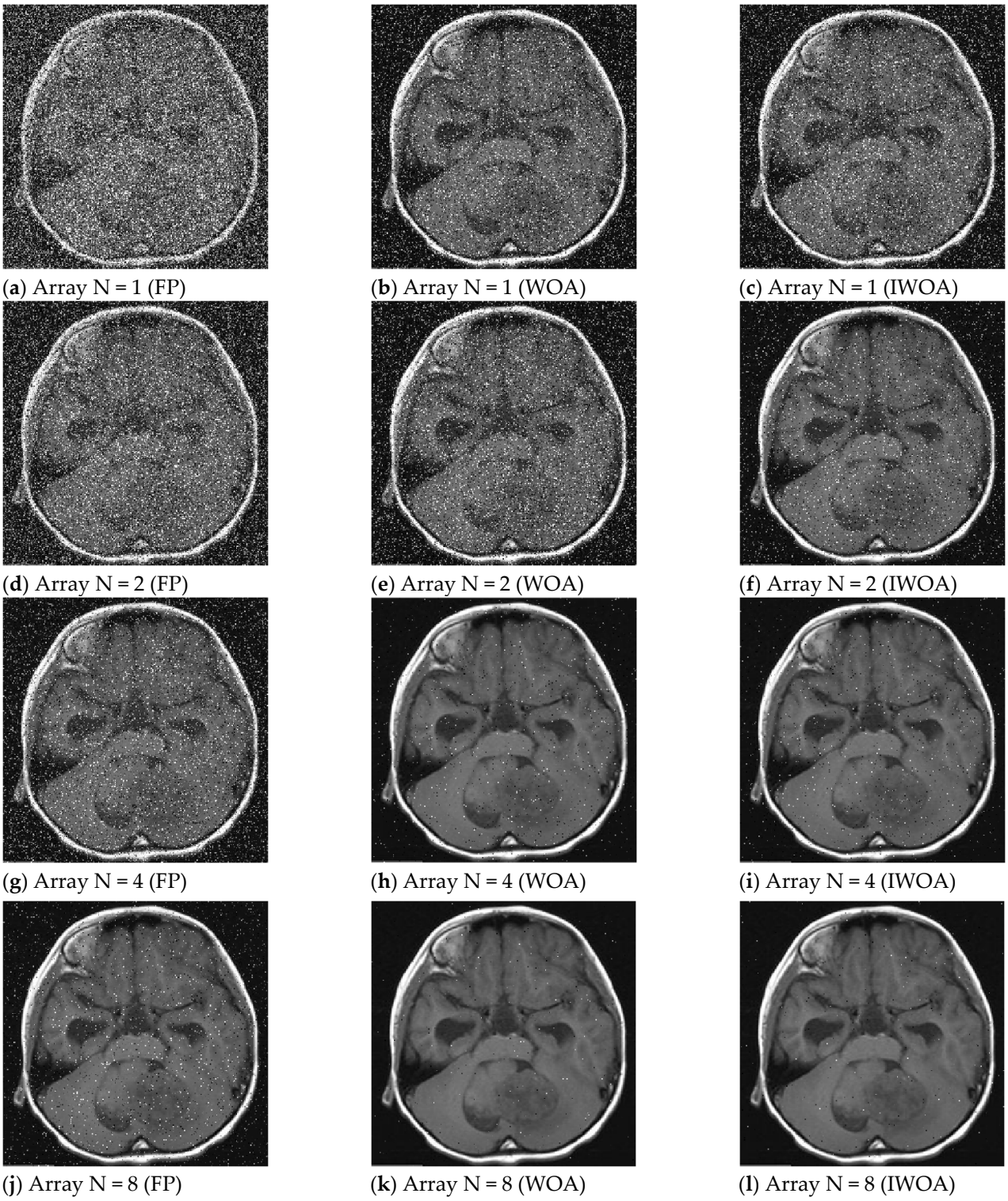

Figure 9. Comparison of denoising effect of MRI image.

6. Conclusions

Aiming at the poor enhancement effect of traditional denoising algorithms on strong noise images, this paper proposes an image denoising algorithm based on improved whale optimization algorithm and parameter adaptive array stochastic resonance, and applies it to the enhancement of noisy images. Firstly, the algorithm converts the gray image into an aperiodic one-dimensional binary pulse amplitude modulation (BPAM) signal by encoding binary symbols and modulating input signals through Hilbert dimensionality reduction

scanning method. Then, the traditional whale optimization algorithm is improved in the initial solution distribution, global search ability and population diversity generalization, and the algorithm is applied to select the structural parameters of stochastic resonance processing module, which effectively improves the adaptive ability of array stochastic resonance model parameters. Finally, the output of the processing module is demodulated, decoded and reverse scanned to acquire the denoised image. Through the image processing simulation experiment of three different styles of images under a strong noise environment, the experiment is respectively compared with four classical filtering methods, the array model method with fixed parameters and the parameter adaptive array model method based on WOA. The experimental results show that, in terms of visual effects, the restored image processed by the image denoising algorithm proposed in this paper is the closest to the original image, which can better show the gray level and image content of the original image. In terms of PSNR value, the PSNR value of the image denoising algorithm proposed in this paper is the largest in different array units. It can be seen that the image denoising algorithm proposed in this paper has a good performance in the restoration effect of the noised image. However, due to the long time consumption of array stochastic resonance, the algorithm proposed in this paper takes a long time in image denoising. At the same time, this paper mainly enhances the image in the strong white Gaussian noise background, but in the actual research, the types of noise are superimposed. In the future research, these two defects will be solved to further improve the performance of the algorithm applied in practice.

Author Contributions: Conceptualization, W.H. and S.J.; methodology, W.H. and S.J.; software, G.Z.; validation, W.H. and G.Z.; formal analysis, W.H.; investigation, S.J. and J.W.; resources, W.H. and G.Z.; data curation, J.W.; writing—original draft preparation, G.Z.; writing—review and editing, W.H.; visualization, W.H. and G.Z.; supervision, W.H., S.J. and J.W.; project administration, W.H. and S.J.; funding acquisition, S.J. All authors have read and agreed to the published version of the manuscript.

Funding: This research is supported by the National Natural Science Foundation (NNSF) of China (NO.62073258, 62003261, 61871318), the Natural Basic Science Research Program of Shaanxi Province of China (NO. 2020JQ-650), and the Scientific Research Program funded by the Shaanxi Education Department (NO. 20JK0788).

Informed Consent Statement: Informed consent was obtained from all subjects involved in the study.

Data Availability Statement: Not applicable.

Conflicts of Interest: The authors declare no conflict of interest.

References

1. Xue, H.Z.; Cui, H.W. Research on image restoration algorithms based on BP neural network. *J. Vis. Commun. Image Represent.* **2019**, *59*, 204–209. [CrossRef]
2. Dastres, R.; Soori, M. Advanced Image Processing Systems. *Int. J. Imaging Robot.* **2021**, *21*, 27–44.
3. Gong, S.; Kumar, R.; Kumutha, D. Design of Lighting Intelligent Control System Based on OpenCV Image Processing Technology. *Int. J. Uncertain. Fuzziness Knowl.-Based Syst.* **2021**, *29*, 119–139. [CrossRef]
4. John, A.; Christian, E.; Glenn, L. Onboard Image-Processing Algorithm for a Spacecraft Optical Navigation Sensor System. *J. Spacecr. Rocket.* **2012**, *49*, 337–352.
5. Chandrasekhar, S.; Laxminarayana, G.; Chakrapani, Y. Novel Hybrid Segmentation Techniques for Cardiac Image Processing in Remote Health Care Monitoring Systems. *J. Med. Imaging Health Inform.* **2017**, *7*, 1153–1159. [CrossRef]
6. Ma, L. Research on distance education image correction based on digital image processing technology. *EURASIP J. Image Video Process.* **2019**, *2019*, 18. [CrossRef]
7. Arsenault, H.H.; Denis, M. Image processing in signal-dependent noise. *Can. J. Phys.* **1983**, *61*, 309–317. [CrossRef]
8. Govinda, D.; Narayanankuttya, K.A.; Govinda, D. Image denoising using total variation wavelet galerkin method. *Procedia Comput. Sci.* **2018**, *143*, 481–492.
9. Archana, K.S.; Sahayadhas, A. Comparison of various filters for noise removal in paddy leaf images. *Int. J. Eng. Technol.* **2018**, *7*, 372. [CrossRef]
10. Awang, N.; Fauadi, M.H.F.M.; Noor, A.Z.M.; Idris, S.A.; Rosli, N.S. An improved image filtering method for weld bead inspection using Unsharp masking technique. *J. Adv. Manuf. Technol.* **2018**, *12*, 341–354.

11. Xu, B.; Jiang, Z.-P.; Wu, X.; Repperger, D.W. Theoretical analysis of image processing using parameter-tuning stochastic resonance technique. In Proceedings of the 2007 American Control Conference, New York, NY, USA, 9–13 July 2007.
12. Yang, Y.B.; Jiang, Z.P.; Xu, B.H.; Daniel, W.R. An investigation of two-dimensional parameter-induced stochastic resonance and applications in nonlinear image processing. *J. Phys. A Math. Theor.* **2009**, *42*, 145207. [CrossRef]
13. Benzi, R.; Parisi, G.; Vulpiani, S.A. A Theory of Stochastic Resonance in Climatic Change. *SIAM J. Appl. Math.* **1983**, *43*, 565–578. [CrossRef]
14. Ye, Q.H.; Huang, H.N.; He, X.Y.; Zhang, C. A SR based radon transform to extra weak lines from noise images. In Proceedings of the 2003 International Conference on Image Processing, Barcelona, Spain, 14–17 September 2003; Volume 1, pp. 849–852.
15. Liu, J.; Li, Z. Binary image enhancement based on aperiodic stochastic resonance. *Image Process. Iet* **2015**, *9*, 1033–1038. [CrossRef]
16. Liu, J.; Hu, B.; Wang, Y.G. Optimum adaptive array stochastic resonance in noisy grayscale image restoration. *Phys. Lett. A* **2019**, *383*, 1457–1465. [CrossRef]
17. Wu, C.Y.; Wu, C.J. Recovery and enhancement of unknown aperiodic binary signal by adaptive aperiodic stochastic resonance. *Pramana* **2021**, *95*, 36. [CrossRef]
18. Wang, G.G.; Gandomi, A.H.; Yang, X.S.; Alavi, A.H. A novel improved accelerated particle swarm optimization algorithm for global numerical optimization. *Eng. Comput.* **2014**, *31*, 1198–1220. [CrossRef]
19. Gao, K.P.; Xu, X.X.; Li, J.B.; Jiao, S.J.; Shi, N. Research on feature enhancement method of weak fault signal of rotating machinery based on adaptive stochastic resonance. *J. Mech. Sci. Technol.* **2022**, *36*, 553–563. [CrossRef]
20. Chi, K.; Kang, J.S.; Tong, R.; Zhang, X.H. An adaptive stochastic resonance method based on multi-agent cuckoo search algorithm for bearing fault detection. *J. Vibroengineering* **2019**, *21*, 1296–1307. [CrossRef]
21. Zhang, X.; Zhang, H.; Guo, J.; Zhu, L.; Lv, S. Research on mud pulse signal detection based on adaptive stochastic resonance. *J. Pet. Sci. Eng.* **2017**, *157*, 643–650. [CrossRef]
22. Paniri, M.; Dowlatshahi, M.B.; Nezamabadi-pour, H. Ant-TD: Ant colony optimization plus temporal difference reinforcement learning for multi-label feature selection. *Swarm Evol. Comput.* **2021**, *64*, 100892. [CrossRef]
23. Paniri, M.; Dowlatshahi, M.B.; Nezamabadi-pour, H. MLACO: A multi-label feature selection algorithm based on ant colony optimization. *Knowl.-Based Syst.* **2020**, *192*, 105285. [CrossRef]
24. Liu, P.H.; Liu, J. Multi-leader PSO (MLPSO): A new PSO variant for solving global optimization problems. *Appl. Soft Comput.* **2017**, *61*, 256–263. [CrossRef]
25. Dowlatshahi, M.B.; Nezamabadi-pour, H. GGSA: A Grouping Gravitational Search Algorithm for data clustering. *Eng. Appl. Artif. Intell.* **2014**, *36*, 114–121. [CrossRef]
26. Serkan, D. A Novel Approach Based on Average Swarm Intelligence to Improve the Whale Optimization Algorithm. *Arab. J. Sci. Eng.* **2022**, *47*, 1763–1776.
27. Mirjalili, S.; Lewis, A. The Whale Optimization Algorithm. *Adv. Eng. Softw.* **2016**, *95*, 51–67. [CrossRef]
28. Huang, W.; Zhang, G.; Jiao, S.; Wang, J. Bearing Fault Diagnosis Based on Stochastic Resonance and Improved Whale Optimization Algorithm. *Electronics* **2022**, *11*, 2185. [CrossRef]
29. Gammaitoni, L.; Hänggi, P.; Jung, P.; Marchesoni, F. Stochastic resonance. *Rev. Mod. Phys.* **1998**, *70*, 223–287. [CrossRef]
30. Leng, Y.G. Mechanism of parameter-adjusted stochastic resonance based on Kramers rate. *Acta Phys. Sin.* **2009**, *58*, 5196–5200. [CrossRef]
31. Duan, F.; Chapeau, B.F.; Abbottt, D. Noise enhanced SNR gain in parallel array of bistable oscillators. *Electron. Lett.* **2006**, *42*, 1008–1009. [CrossRef]
32. Watkins, W.A.; Schevill, W.E. Aerial Observation of Feeding Behavior in Four Baleen Whales: Eubalaena glacialis, Balaenoptera borealis, Megaptera novaeangliae, and Balaenoptera physalus. *J. Mammal.* **1979**, *60*, 155–163. [CrossRef]
33. Mehne, H.H.; Mirjalili, S. A parallel numerical method for solving optimal control problems based on whale optimization algorithm. *Knowl.-Based Syst.* **2018**, *151*, 114–123. [CrossRef]
34. Bi, X.J.; Li, Y.; Chen, C.Y. A self-adaptive teaching-and-learning-based optimization algorithm with a mixed strategy. *J. Harbin Eng. Univ.* **2016**, *37*, 842–848.
35. He, Q.; Lin, J.; Xu, H. Hybrid Cauchy Mutation and Uniform Distribution of Grasshopper Optimization Algorithm. *Control. Decis.* **2021**, *36*, 1558–1568.
36. Wang, S.; Xu, X.-S. A New Algorithm of Hilbert Scanning Matrix and its MATLAB Program. *J. Image Graph.* **2006**, *11*, 119–122.
37. Gonzalez, R.C.; Woods, R.E.; Eddins, S.L. Digital Image Processing Using Matlabtm. *Digit. Image Process. Using Matlab.* **2004**, *21*, 197–199.
38. Zhao, J.; Ma, Y.; Pan, Z.; Zhang, H. Research on Image Signal Identification Based on Adaptive Array Stochastic Resonance. *Syst. Sci. Complex.* **2022**, *35*, 179–193. [CrossRef]